

## MINIREVIEW

[View Article Online](#)  
[View Journal](#) | [View Issue](#)Cite this: *Chem. Sci.*, 2020, **11**, 4287

All publication charges for this article have been paid for by the Royal Society of Chemistry

Received 27th November 2019  
Accepted 4th March 2020

DOI: 10.1039/c9sc06006e

[rsc.li/chemical-science](http://rsc.li/chemical-science)

## Recent developments in nickel-catalyzed intermolecular dicarbofunctionalization of alkenes

Joseph Derosa, Omar Apolinar, Taeho Kang, Van T. Tran and Keary M. Engle \*

Nickel-catalyzed three-component alkene difunctionalization has rapidly emerged as a powerful tool for forging two C–C bonds in a single reaction. Building upon the powerful modes of bond construction in traditional two-component cross-coupling, various research groups have demonstrated the versatility of nickel in enabling catalytic 1,2-dicarbofunctionalization using a wide range of carbon-based electrophiles and nucleophiles and in a fully intermolecular fashion. Though this area has emerged only recently, the last few years have witnessed a proliferation of publications on this topic, underscoring the potential of this strategy to develop into a general platform that offers high regio- and stereoselectivity. This minireview highlights the recent progress in the area of intermolecular 1,2-dicarbofunctionalization of alkenes *via* nickel catalysis and discusses lingering challenges within this reactivity paradigm.

## Introduction

Transition-metal-catalyzed cross-coupling has served as a powerful engine for the rapid build-up of molecular complexity through C–C bond formation using organohalides and organometallic reagents.<sup>1,2</sup> Despite the efficiency of different transition metal catalysts, including palladium, nickel, and copper, in mediating C(sp<sup>2</sup>)–C(sp<sup>2</sup>) bond formation, C(sp<sup>3</sup>)–X and C(sp<sup>3</sup>)–M reagents have only recently become viable coupling partners with advances in mechanistic understanding and catalyst design.<sup>3</sup> A central challenge when using C(sp<sup>3</sup>) coupling partners is the propensity of the resulting alkylmetal intermediate to undergo β-hydride elimination, generating a highly reactive metal–hydride that can take part in various off-cycle pathways that preclude the desired C–C bond-forming event. To suppress β-hydride elimination in two-component cross-couplings, different approaches have been pursued, including developing effective ligand scaffolds and employing transition metals that are resistant to β-hydride elimination, such as nickel.<sup>4</sup> Indeed, several recent developments in nickel-catalyzed C(sp<sup>3</sup>)–C(sp<sup>3</sup>) cross-coupling have taken advantage of the unique characteristics of nickel compared to palladium, such as faster rates for oxidative addition and migratory insertion, sluggish rates for β-hydride elimination and propensity to engage in single-electron transfer (SET), to enable otherwise difficult transformations.<sup>5</sup>

Decades of development in the cross-coupling arena have yielded a highly modular toolkit for bond construction in organic synthesis. Nevertheless, the introduction of an alkene as a third component has only recently emerged as a viable

catalytic strategy.<sup>6</sup> In these transformations, two carbogenic fragments are delivered across the C=C bond, resulting in 1,2-dicarbofunctionalization. These reactions are often referred to as “conjunctive cross-coupling” in the literature due to the integration of a third “conjunctive” component that can interlink with the two familiar fragments used in classical cross-couplings. Such methods offer strategic advantages in synthesis yet present several interrelated challenges in selectivity control. As such, they are at the forefront of modern catalysis research.

As with two-component cross-couplings, nickel offers advantages as a catalyst in intermolecular 1,2-dicarbofunctionalization of alkenes, namely: increased resistance to β-hydride elimination, increased propensity for oxidative addition, and ability to react with radical intermediates. These properties are ideal for preventing undesired chain-walking processes in alkene functionalization and expanding the scope of compatible coupling partners. This minireview focuses on the recent flurry of developments in nickel-catalyzed intermolecular 1,2-dicarbofunctionalization of alkenes (Scheme 1). Mechanistically, this family of reactions involves a shared sequence of elementary steps. First the alkene substrate is intercepted with an initial coupling partner (C–Y) in a net carbometallation which is followed by incorporation of the second coupling partner (C–Z) *via* association to the metal and reductive elimination. In most cases, a transmetalating agent (*i.e.*, C–B(OR)<sub>2</sub> or C–ZnX) is used to incorporate one of the carbon fragments. However, reductive couplings involving two electrophiles will also be discussed. An important aspect of this family of reactions is the difficulty of achieving high levels of regio-, stereo-, and chemoselectivity. In most cases, this is dependent on the mechanism by which the nickel catalyst interacts with the coupling partners (single- or two-electron processes) and the alkene carbometallation pathway (*syn*- or

Department of Chemistry, The Scripps Research Institute, 10550 North Torrey Pines Road, La Jolla, California 92037, USA. E-mail: [keary@scripps.edu](mailto:keary@scripps.edu)



Scheme 1 General scheme depicting nickel-catalyzed intermolecular 1,2-dicarbonylfunctionalization of alkenes.

*anti*-insertion). While the intricacies of the reaction mechanisms will be described for individual reactions highlighted below, these transformations typically proceed *via* one of two main pathways for carbometallation: (A) *syn*-1,2-migratory insertion of the organonickel species directly into the C–C  $\pi$ -bond, or (B) single-electron transfer-initiated radical addition to the C–C  $\pi$ -bond followed by radical recombination of the resulting alkyl radical to produce an organonickel species.

This review is organized based on the type of alkene employed: (1) acrylate-type substrates, (2) heteroatom-substituted alkenes, (3) styrenes, (4) strained alkenes, and (5) non-conjugated (and unstrained) alkenes (Scheme 2). Across the examples that are covered, we emphasize different strategies that prevent  $\beta$ -hydride elimination and control regioselectivity, noting that in many cases multiple effects operate in concert to enable the transformation. Furthermore, we highlight the different types of carbon-based coupling partners used, and include insights on the specific redox manifold of the nickel



Scheme 2 Organization of topics in this review based on alkene substrate and stabilization strategy.

catalyst in the reaction. 1,2-Dicarbonylfunctionalization using other transition metals<sup>7</sup> and nickel-catalyzed intramolecular 1,2-dicarbonylfunctionalization<sup>8</sup> are beyond the scope of this article and will not be discussed. Overall, this minireview serves to showcase exciting developments in this area and to discuss current limitations, challenges, and opportunities moving forward.

## Acrylate-type substrates

Conjugated alkenes such as acrylates can readily undergo Giese addition with radical coupling partners usually leading to hydrofunctionalized products. However, the generated secondary alkyl radical intermediates can alternatively be trapped with organonickel species en route to 1,2-dicarbonylfunctionalization. In 2016, Baran and coworkers demonstrated one of the first examples of nickel-catalyzed intermolecular 1,2-dicarbonylfunctionalization using benzyl acrylate, redox-active esters (RAEs), and phenyl zinc halide salts as transmetalating agents (Fig. 1).<sup>9</sup> Using 20 mol%  $\text{NiCl}_2 \cdot \text{glyme}$  with 40 mol% bipyridyl ligand **L1**, a wide range of tertiary alkyl RAEs including heterocycles, strained carbocycles, and heteroatom-containing alkyl chains are tolerated. The authors propose an initial SET that results in decarboxylation to generate a tertiary alkyl radical. This radical can engage with benzyl acrylate in a Giese-type fashion, followed by radical recombination with the aryl nickel species generated *in situ*. The resulting  $\text{Ni}(\text{Ar})(\text{alkyl})$  species undergoes reductive elimination to yield the desired 1,2-dicarbonylfunctionalized product.

In 2017, the Nevado lab reported a reductive 1,2-arylalkylation method. Compatible alkenes included various acrylate-type substrates (Fig. 2A), as well as three classes of allylic compounds (not shown).<sup>10</sup> The authors employed 10 mol%  $\text{NiCl}_2(\text{py})_4$  and 10 mol% bipyridyl ligand **L1** with aryl iodides and tertiary alkyl iodides using tetrakis(dimethylamino)ethylene (TDAE) as the reductant. Various control experiments such as radical-traps shed light on the radical-based nature of the reaction mechanism and the capability of TDAE in reducing  $\text{Ni}(\text{II})$  to low-valent nickel species under the reaction conditions. The authors propose a catalytic cycle involving the reduction of  $\text{Ni}(\text{II})$  to  $\text{Ni}(\text{0})$  using TDAE which can then undergo disproportionation to yield  $\text{Ni}(\text{I})$  (Fig. 2B). This  $\text{Ni}(\text{I})$  species engages in SET with the corresponding alkyl halide, generating an alkyl radical that

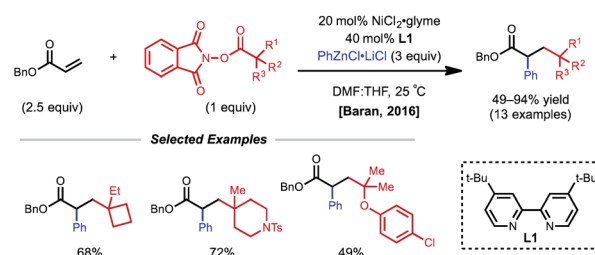


Fig. 1 1,2-Dicarbonylfunctionalization of benzyl acrylate using phenyl zinc chloride and RAEs.

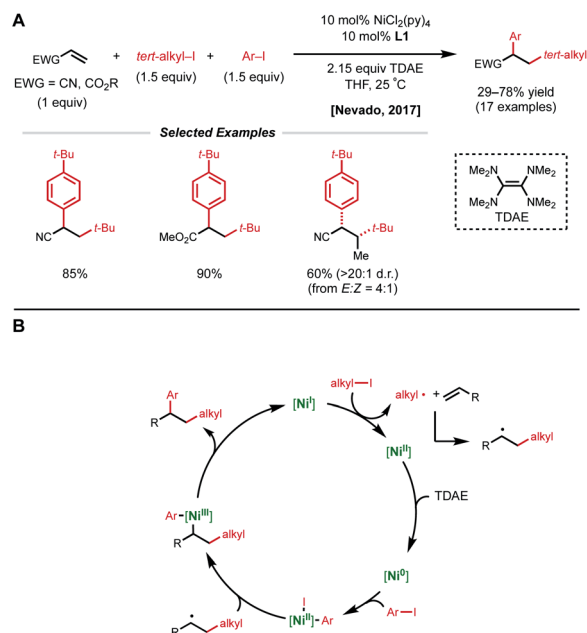


Fig. 2 (A) Reductive 1,2-dicarbofunctionalization of acrylate-type compounds. (B) Proposed catalytic cycle.

performs radical addition to the alkene substrate generating a new secondary alkyl radical. The newly formed Ni(II) species undergoes a second reduction event by TDAE to yield Ni(0) that can perform oxidative addition to the aryl halide coupling partner. The Ni(II)-aryl species is then intercepted by the secondary alkyl radical generated in the earlier step, resulting in a secondary alkyl Ni(III)-aryl that undergoes a facile reductive elimination to regenerate Ni(I) and close the catalytic cycle. In 2019, Nevado and coworkers expanded this reductive 1,2-alkylation reaction to a variety of terminal non-conjugated alkenes.<sup>11</sup>

## Heteroatom-substituted alkene substrates

The presence of a heteroatom on an alkene provides electronic stabilization of a Ni(II) or  $\alpha$ -radical intermediate, allowing for facile 1,2-dicarbofunctionalization. In 2016, Zhang and coworkers reported a 1,2-difluoroalkylation reaction of enamides using aryl boronic acids and difluoroalkyl bromides (Fig. 3).<sup>12</sup> This reaction employs 5 mol% NiCl<sub>2</sub>·glyme with 5 mol% bipyridyl ligand L2 and showcases a broad scope for both coupling partners. The alkene scope is limited to terminal *N*-vinyl-pyrrolidinones; and closely related substrates; for example, the corresponding oxazolidinone, phthalimide, and acyclic acetamide<sup>13</sup> also react to deliver the desired products. The authors performed radical clock experiments that provide evidence for the presence of radical species in related systems. The authors propose that there is a directing effect from the carbonyl group (*via* a four-membered nickelacycle intermediate). Modest enantioselectivity is achieved using a chiral diamine ligand in a single

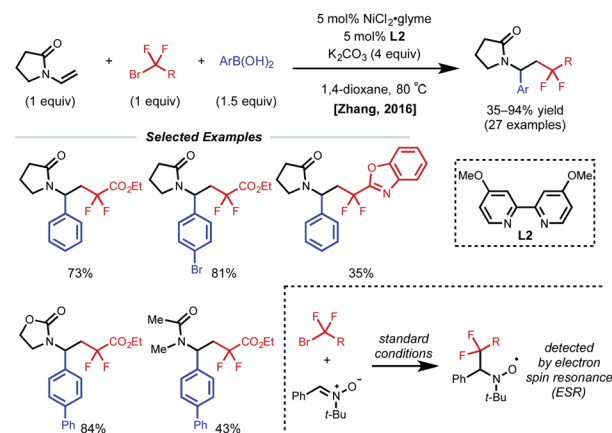


Fig. 3 1,2-Difluoroalkylation of enamides.

example (18% ee). In 2019, the Zhang group developed a complementary 1,2-difluoroalkylation reaction using the same substrate class with dialkyl zinc reagents.<sup>14</sup> In this report, the authors conduct the reaction with an *N*-vinyl pyrrolidine and do not observe reactivity, supporting a nickel-chelation hypothesis. Later in 2019, the Morken group reported an asymmetric 1,2-dialkylation and 1,2-arylation of alkenyl boronic acid pinacol esters (BPin) (Fig. 4A).<sup>15</sup> Taking advantage of the stability of the  $\alpha$ -boryl radical,<sup>16</sup> alkyl zinc halides and tertiary alkyl halides are effective coupling partners using 10 mol% NiBr<sub>2</sub>·glyme and 13 mol% chiral diamine ligand L3. Interestingly, the use of pinacol as boron protecting group was necessary to achieve high ee. Based on earlier precedents invoking radical species in nickel-catalyzed cross-coupling and simple TEMPO inhibition experiments, the authors conclude that this reaction likely proceeds through a radical-addition-based mechanism (Fig. 4B). Since this report, alkenyl boron reagents have proven to be highly versatile conjunctive reagents, particularly when employed under dual nickel/photoredox catalysis.<sup>17</sup> Also, it is appropriate to note that similar 1,2-dicarbofunctionalized products can also be obtained *via* nickel-catalyzed metalate rearrangement pathways.<sup>18</sup>

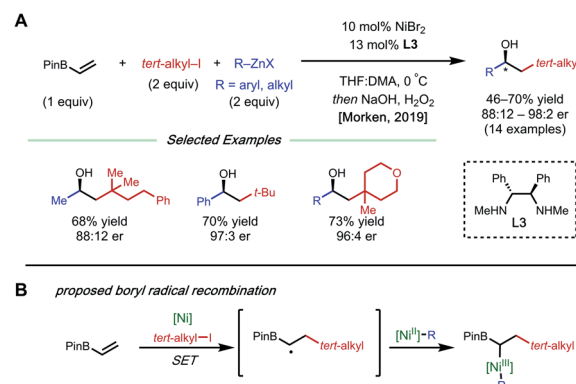
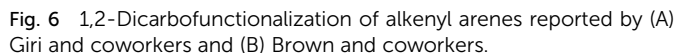


Fig. 4 (A) Asymmetric 1,2-dicarbofunctionalization of vinyl-Bpin. (B) Proposed mechanism.

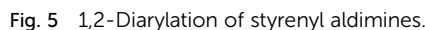


Only one year later, both the Giri and Brown labs reported 1,2-dicarbofunctionalization reactions of vinyl arenes without the use of a directing group. The Giri group employed 5 mol% NiBr<sub>2</sub> with primary/secondary alkyl halides (or 5 mol% NiCl<sub>2</sub>(PPh<sub>3</sub>)<sub>2</sub> with tertiary alkyl halides) and aryl zinc reagents for 1,2-alkylarylation of terminal vinyl arenes (Fig. 6A).<sup>21</sup> Mechanistic experiments established that Ni(II) is reduced to Ni(0) *in situ* by the excess aryl zinc reagent and that radicals are present throughout the course of the reaction, supporting a radical addition pathway. Reaction progress kinetic analysis revealed positive order kinetics in the alkyl halide coupling partner, suggesting its involvement in the rate-determining step. Giri and coworkers also reported the utility of this method toward the synthesis of FLAP inhibitors.<sup>22</sup>



The Brown lab simultaneously reported a 1,2-diarylation of terminal and internal vinyl arenes using 7.5 mol% NiCl<sub>2</sub> with aryl bromides and aryl boronic acid neopentyl glycol esters (ArB(nep)) (Fig. 6B).<sup>23</sup> It is important to note that internal conjugated substrates were tolerated and gave desired products with high regio- and stereoselectivity. The authors propose a *syn*-insertion mechanism, which is supported by the formation of a single diastereomer with a cyclic internal substrate. Interestingly, 0.1 equiv. of B<sub>2</sub>Pin<sub>2</sub> is utilized for the reduction of Ni(II) to Ni(0). In addition, the reaction is highly scalable and was applied in the synthesis of *rac*-lasofoxfene.

Despite the rapid growth in this area, the identification of a suitable asymmetric variant of this 1,2-dicarbonyl functionalization cascade remained elusive. In 2019, Diao and coworkers developed the first nickel-catalyzed asymmetric reductive 1,2-homodimerization of styrenes.<sup>24</sup> In this reaction manifold, 10 mol% NiBr<sub>2</sub>·glyme, 20 mol% chiral bi-oxazoline **L4**, 8 mol% ABNO additive, excess aryl bromide, and zinc dust generated the desired homo-dimerization product in high ee (Fig. 7A). Interestingly, an *N*-oxyl radical additive was found to be crucial for obtaining high ee. Though the authors do not explicitly discuss the role of the additive, they propose that it may act as a ligand on the Ni-catalyst at some point given the importance of the near 1 : 1 ratio of ABNO : Ni. The choice of ligand **L4** was also critical to achieving the desired reactivity and stereocontrol, with more common ligands in asymmetric nickel catalysis resulting in low or negligible ee.





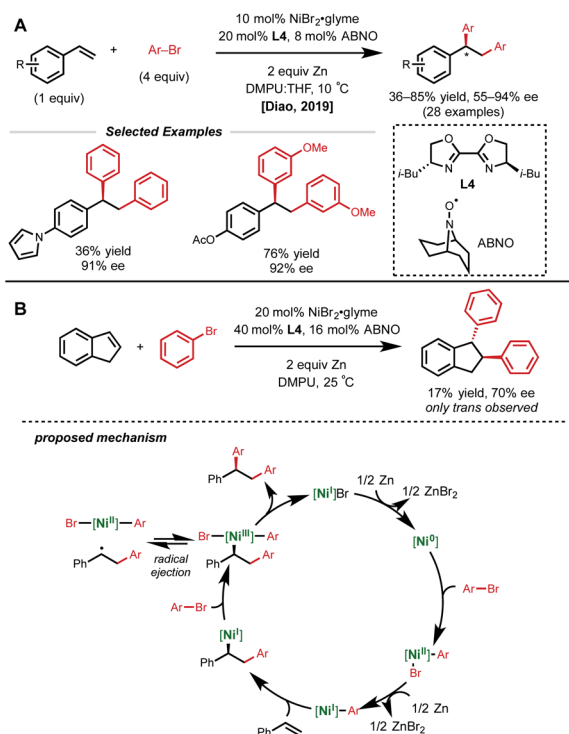


Fig. 7 (A) Asymmetric reductive 1,2-homodiarylation of vinyl arenes. (B) Key mechanistic experiment and proposed catalytic cycle.

Several experiments were conducted to help elucidate the mechanistic underpinnings of this nickel-catalyzed asymmetric 1,2-diarylation (Fig. 7B). The authors first examined the Ni/ligand ratio and observed a linear correlation, indicating that there is likely one equivalent of ligand on nickel in the enantiodetermining step. Additionally, indene was subjected to the reaction conditions and only the *trans* product was obtained in 70% ee. The authors conclude that this may be evidence of an initial *syn*-insertion followed by reversible radical ejection that selectively scrambles the stereochemistry, positioning nickel on the less hindered face. Other experiments pointing to radical species included the inhibition of the reaction by excess ABNO, and the detection of benzylic homodimers, albeit in low yield (2%).

## Strained alkenes

Strained alkenes, such as norbornene, undergo strain release upon migratory insertion or radical addition, furnishing conformationally constrained alkylnickel intermediates that cannot readily undergo requisite C–C bond rotation to allow  $\beta$ -H elimination. As a consequence, these substrates are also competent in 1,2-dicarbofunctionalization under nickel catalysis. In 2019, Stanley and coworkers reported a *syn*-selective intermolecular 1,2-carboacylation procedure with norbornenes, *N,N*-substituted benzamide electrophiles, and tetraarylboron nucleophiles (Fig. 8).<sup>25</sup> The transformation was found to take place under the action of 10 mol% Ni(cod)<sub>2</sub> and 2 equiv. of H<sub>3</sub>BO<sub>3</sub>, tolerating a wide array of norbornene-type alkenes and

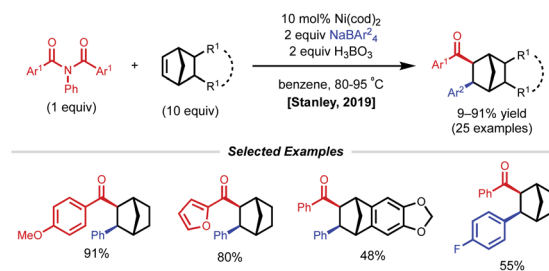


Fig. 8 1,2-Carboacylation of norbornenes.

coupling partners. The proposed catalytic cycle begins with oxidative addition of the Ni(0) catalyst to *N,N*-substituted benzamide, which affords a Ni(II)(acyl)(amido) species. Migratory insertion of norbornene to the Ni(II)(acyl)(amido) species forms a Ni(II)(alkyl)(amido) species. Subsequent transmetalation with *in situ* formed triarylborane generates a Ni(II)(alkyl)(aryl) species. Finally, reductive elimination turns over the catalytic cycle and forms the 1,2-carboacylated product.

## Non-conjugated alkene substrates

In acyclic, unactivated alkenes, selective intermolecular 1,2-dicarbofunctionalization becomes a significant challenge. Despite the value of employing non-conjugated alkenes as starting materials, achieving desired reactivity is mired by two main factors: (1) migratory insertion is more difficult and (2) undesired  $\beta$ -hydride elimination is more prevalent. While overcoming these obstacles may seem daunting, various groups have made significant progress in providing a general platform for nickel-catalyzed 1,2-dicarbofunctionalization of non-conjugated alkenes.

In 2017, Engle and coworkers implemented a directing group strategy to achieve regio- and diastereoselective 1,2-aryllalkylation of  $\beta,\gamma$ -unsaturated alkenyl carbonyl compounds (Fig. 9A).<sup>26</sup> Using a removable 8-aminoquinoline (AQ) bidentate auxiliary, a wide range of internal and  $\alpha$ -substituted substrates could be effectively difunctionalized with organozinc reagents and aryl iodides using 10 mol% Ni(cod)<sub>2</sub>. Internal alkenes give a single diastereomer, suggesting that a *syn*-insertion mechanism is operative. Initial oxidative addition to the aryl iodide generates an arylnickel(II) intermediate that can coordinate AQ and undergo *syn*-insertion with the pendant alkene, placing the aryl fragment at the  $\gamma$ -position. The authors propose that the bidentate auxiliary is key to enabling this reactivity, resulting in a five-membered nickelacycle after insertion that is less prone to  $\beta$ -hydride elimination (Fig. 9B). At this stage, transmetalation with organozinc and reductive elimination yields the desired product. After the desired 1,2-difunctionalization, these products could undergo hydrolysis to remove the AQ auxiliary and unmask the free carboxylic acid.

Using a similar directing group strategy, the Engle laboratory reported a 1,2-dialkylation in 2018 using alkyl zinc reagents and alkyl halides, marking the first example of differentiable 1,2-dialkylation of non-conjugated alkenes (Fig. 10).<sup>27</sup> While the standard AQ-substrate remained the same, this reaction gave





Fig. 9 (A) Directed 1,2-arylalkylation of  $\beta,\gamma$ -unsaturated alkenyl carbonyl compounds. (B) Key mechanistic experiment and proposed catalytic cycle.

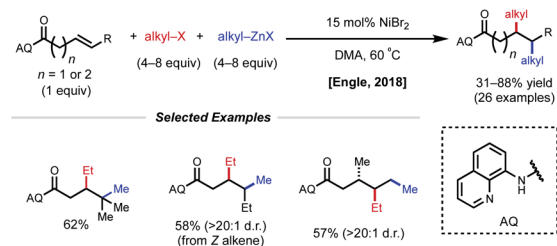


Fig. 10 Directed 1,2-dialkylation of  $\beta,\gamma$ - and  $\gamma,\delta$ -unsaturated alkenyl carbonyl compounds.

the opposite regioselectivity (alkyl nucleophile at the  $\gamma$ -position) compared to the previous report in which aryl iodides were used as the electrophilic coupling partner. Interestingly, this reaction tolerates an even broader range of alkene coupling partners, including trisubstituted and extended chain  $\gamma,\delta$ -unsaturated alkenes. Similarly, only a single diastereomer was detected in the case of internal alkenes, suggesting a *syn*-insertion mechanism. Radical-trap experiments shed light on the potential for radical species to be involved in catalysis. The authors suggest that this reaction operates through a SET pathway with different redox at nickel compared to the earlier example ( $\text{Ni(I)}/\text{Ni(III)}$ ) vs.  $\text{Ni(0)}/\text{Ni(II)}$ ) based on the abundance of  $\text{Ni(I)}/\text{Ni(III)}$  precedent in the context of  $\text{C(sp}^3\text{)}\text{-X}$  cross-coupling literature. A plausible mechanism involving the intermediacy of  $\text{Ni(I)}$  is proposed. First, transmetalation/carbometallation yields a putative chelated nickelacycle. A subsequent SET event with the alkyl

halide followed by radical recombination and reductive elimination gives the desired product. This SET mode of nickel catalysis using AQ-bound substrates was later extended to a complementary 1,2-carboamination system.<sup>28</sup> Very recently, the Lin and Yao groups applied this AQ-directed system toward a reductive 1,2-dialkynylation of non-conjugated alkenes.<sup>29</sup>

In 2018, the Zhao group reported a series of 1,2- and 1,3-dicarbofunctionalization reactions using a 2-aminopyrimidine directing group derived from allyl amine with  $\text{C(sp}^2\text{)}/\text{C(sp}^2\text{)}\text{-X}$  electrophiles and  $\text{C(sp}^2\text{)}\text{-boronic acids}$  as nucleophiles (Fig. 11).<sup>30</sup> In this case, the regioselectivity of the reaction was based on the combination of electrophile/nucleophile. For example, vinyl bromide electrophiles led to incorporation of the electrophile at the terminal position, and alkynyl halides lead to incorporation of the electrophile at the internal position. Interestingly, the use of an aryl electrophile led exclusively to 1,3-dicarbofunctionalized products, pointing to the challenge associated with  $\beta$ -hydride elimination. *N*-Allyl benzamides were shown to be compatible substrates in 1,2-alkynylation.

In 2018, the Giri lab extended their imine-directed diarylation reaction using aryl zinc reagents and aryl halides to linear, non-conjugated terminal alkenes (Fig. 12). In their initial attempt to obtain the desired  $\gamma,\delta$ -diarylated products, only undesired Heck product was observed. Upon modifying reaction conditions, they found that 1,3-dicarbofunctionalization is possible with 5 mol%  $\text{NiBr}_2$  catalyst and 5 mol%  $(\text{PhO})_3\text{P}$  as ligand (Fig. 12A).<sup>31</sup> The authors propose that reduction of the  $\text{Ni(II)}$  species to  $\text{Ni(0)}$  by the aryl zinc reagent occurs first. After oxidative addition and coordination to the alkene and imine directing group by the nickel center, the phosphite ligand facilitates the contraction of the transient 6-membered nickelacycle to a 5-membered nickelacycle *via* a  $\beta$ -hydride elimination/ $\text{Ni-H}$  reinsertion event. Lastly, transmetalation and reductive elimination afford the reported  $\beta,\delta$ -diarylketoones. Following this report, the Giri lab developed a complementary method to achieve  $\gamma,\delta$ -diarylketoone products (Fig. 12B).<sup>32</sup> In this case, 5 mol%  $\text{Ni(cod)}_2$  catalyst without ancillary ligand was employed; however,  $\text{AgBF}_4$  or  $\text{CuI}$  were crucial halide scavenger additives. The authors claim that the abstraction of halide ligand from  $\text{Ni(II)}$  after the oxidative addition step produces a cationic aryl nickel species that can readily undergo migratory insertion, transmetalation, and reductive elimination without undergoing  $\beta$ -hydride elimination. In 2019, Giri reported a similar 1,3-dicarbofunctionalization using more weakly



Fig. 11 Divergent regioselectivity in 1,2-dicarbofunctionalization of allyl amines using pyrimidine directing groups.



Fig. 12 (A and B) Imine-directed 1,3- and 1,2-diarylation of  $\gamma,\delta$ -unsaturated ketimines. (C) 1,3-Vinylarylation of  $\gamma,\delta$ -unsaturated  $\alpha$ -cyanoesters.

coordinating alkenyl cyanoesters as substrates with vinyl triflates and diaryl zinc reagents as coupling partners (Fig. 12C).<sup>33</sup> The optimal conditions for this  $\beta,\delta$ -vinylarylation use 5 mol%  $\text{NiCl}_2$  and 1.5 equiv. of both  $\text{KPF}_6$  and 4-phenylpyridine (4-PhPy). The authors postulate a  $\text{Ni}(\text{I})/\text{Ni}(\text{III})$  catalytic cycle where  $\text{NiCl}_2$  is first reduced to a cationic  $\text{Ni}(\text{I})$  species that is bound to the substrate and 4-PhPy. Transmetalation with  $\text{Ar}_2\text{Zn}$  then fosters a neutral  $\text{Ni}(\text{I})$  species, allowing alkene insertion to subsequently occur. Next, the anionic 6-membered  $\text{Ni}(\text{I})$ -enolate metallacycle contracts to form an anionic 5-membered  $\text{Ni}(\text{I})$ -enolate metallacycle *via* a  $\beta$ -hydride elimination/ $\text{Ni}$ -H reinsertion sequence. Oxidative addition to the vinyl triflate electrophile and subsequent reductive elimination yields the  $\beta,\delta$ -vinylarylated products.

A more general radical addition strategy toward reacting allylic carbonates with acyl chlorides and perfluoroalkyl halides in a reductive manifold was employed by Chu and coworkers in 2018 (Fig. 13A).<sup>34</sup> Key to the success of this reaction was the careful positioning of a coordinating group in the substrate to allow for the generation of a stabilized 6-membered nickelacycle upon radical recombination. A series of mechanistic studies including substrate modification and TEMPO experiments support the directing group effect and radical addition pathway, respectively. The authors propose a catalytic cycle similar to that of the Nevado group.<sup>10</sup> First, SET from low-valent nickel

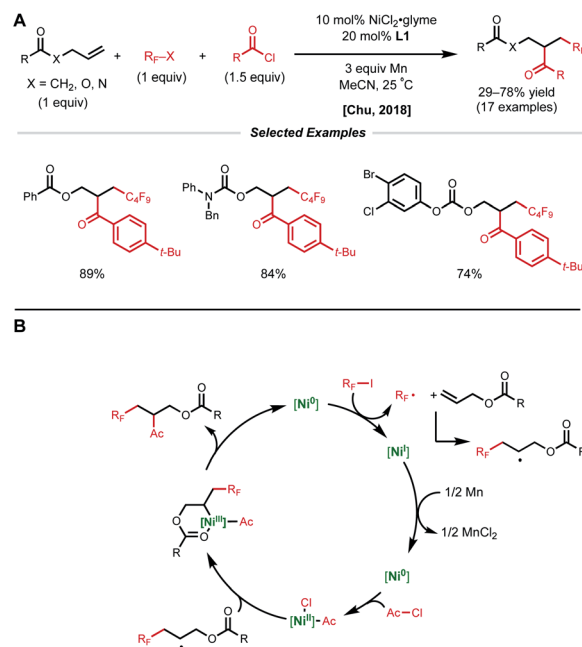


Fig. 13 (A) Reductive 1,2-perfluoroalkylacylation of allylic substrates. (B) Proposed catalytic cycle.

generates a perfluoroalkyl radical that adds to the allylic substrate (Fig. 13B). This newly generated secondary alkyl radical recombines with a  $\text{Ni}(\text{II})$ -acyl intermediate to form a secondary  $\text{Ni}(\text{III})$ (alkyl)(acyl) species that is stabilized by substrate coordination to allow for productive reductive elimination.

Concurrent with these developments in 2018, the Engle laboratory reported a conjunctive cross-coupling method of  $\beta,\gamma$ - and  $\gamma,\delta$ -unsaturated alkenyl amides with native monodentate amide functional groups instead of strong bidentate auxiliaries (Fig. 14).<sup>35</sup> Using 15 mol%  $\text{Ni}(\text{cod})_2$  with dimethyl fumarate (dmfu), an electron-deficient olefin (EDO) ligand, a wide range of aryl boronic acid neopentyl glycol esters and aryl iodides could be incorporated. Additionally, a broad scope of amides was tolerated including allyl amines with carbonyl-containing protecting groups. The authors propose a  $\text{Ni}(\text{0})/\text{Ni}(\text{II})$  mechanism analogous to that of the examples above. Experimental and computational evidence suggests that the substrate binds the nickel catalyst at the carbonyl oxygen rather than the amide



Fig. 14 Simple amide-directed 1,2-diarylation.



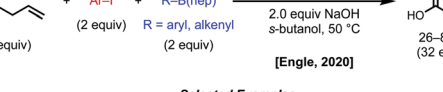
Reaction scheme showing the asymmetric allylation of a chiral auxiliary (Het) with ZnMe<sub>2</sub> and an α,β-unsaturated ketone (AcO-CH=CH-R) catalyzed by 10 mol% NiBr<sub>2</sub>(glyme) at -40 to 0 °C, yielding 15–99% (45 examples).

**Selected Examples**

Three examples of the reaction are shown:

- Example 1: Yield 36%, >20:1 d.r.<sup>a</sup> (2.5:1 d.r.<sup>b</sup>)
- Example 2: Yield 78%
- Example 3: Yield 80%


**A**



(1 equiv) + Ar-I (2 equiv) + R-B(neop) (2 equiv)  $\xrightarrow[2.0 \text{ equiv NaOH, } s\text{-butanol, } 50^\circ\text{C}]{15 \text{ mol\% Ni(cod)}_2}$  HO-CH(allyl)-CH(R)-COOAr (26-86% yield (32 examples))

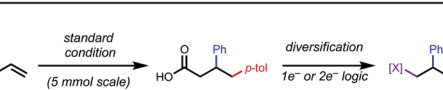
[Engle, 2020]

**Selected Examples**



71%      83%      28% (>20:1 d.r.) (from Z alkene)

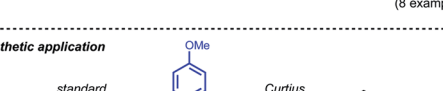
**B**



HO-CH(allyl)-CH(Ph)-COOAr  $\xrightarrow[\text{(5 mmol scale)}]{\text{standard condition}}$  HO-CH(allyl)-CH(Ph)-COOAr  $\xrightarrow[1e^- \text{ or } 2e^- \text{ logic}]{\text{diversification}}$  [X]-CH(allyl)-CH(Ph)-COOAr

80% (1.02 g)      [X] = CH<sub>2</sub>OAr, aryl, alkenyl, B(pin)... (8 examples)

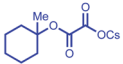
**synthetic application**



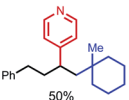
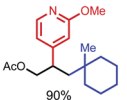
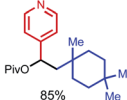
HO-CH(allyl)-CH(Ph)-COOAr  $\xrightarrow{\text{standard condition}}$  HO-CH(allyl)-CH(Ph)-COOAr  $\xrightarrow{\text{Curtius rearrangement}}$  TRPV1 antagonist

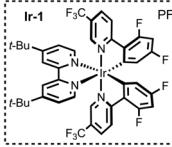
61%

**A**

$R-CH=CH_2$  (1 equiv) + (Het)aryl-I (2 equiv) +  (2 equiv)  $\xrightarrow[\text{60 mol\% Ir-1, 20 mol\% NiCl}_2\cdot\text{DME, 20 mol\% dtbbpy}]{\text{DMSO, 35 }^\circ\text{C, 90 W blue LED}}$   $R-CH_2-CH_2-CH_2-$  (34–92% yield, 31 examples)

**Selected Examples**

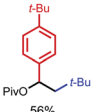
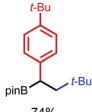
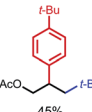
 50%  
 90%  
 85%

**Ir-1** 

**B**

$R-CH=CH_2$  (1.5 equiv) + Ar-I (1 equiv) + alkyl-[Si] (1.5 equiv)  $\xrightarrow[\text{34 W blue LED}]{\text{DMF, 30 }^\circ\text{C}}$   $R-CH_2-CH_2-CH_2-$  (15–74% yield, 22 examples)

**Selected Examples**

 56%  
 74%  
 45%



when subjected to the reaction conditions with either stoichiometric or catalytic amounts of **Ir-1** catalyst. From these results, Chu and coworkers propose that the mechanism begins with formation of a tertiary alkyl radical *via* the oxidation of the oxalate by the photoexcited **Ir-1** catalyst. The tertiary alkyl radical then adds onto the alkene forming a secondary alkyl radical, which is captured by the Ni(0) species to form an alkyl-Ni(I) intermediate. Oxidative addition of the alkyl-Ni(I) intermediate with an aryl halide generates an alkyl-Ni(III)-aryl intermediate. The high valent Ni(III) species undergoes rapid reductive elimination to afford the 1,2-alkylarylated product and Ni(I)-Br. Reduction of the Ni(I)-Br species by Ir(II) regenerates the ground-state **Ir-1** catalyst, closing the dual catalytic cycles.

Concurrent work under the same photocatalytic paradigm was done by the Nevado group to accomplish 1,2-alkylarylation of alkenes (Fig. 17B).<sup>39</sup> Although most substrates are conjugated alkenes, a handful of non-conjugated alkenes are also viable. This transformation is achieved using aryl iodides, alkyl silicates, 1 mol% Ru(bpy)<sub>3</sub>Cl<sub>2</sub>·6H<sub>2</sub>O, 10 mol% NiCl<sub>2</sub>·6H<sub>2</sub>O, and 10 mol% dtbpy (**L1**) with irradiation by 34 W blue LED light. Under the optimized reaction conditions, non-conjugated alkenes such as vinyl pivalate, vinyl boronic acid pinacol ester, and allyl acetate using tertiary alkyl silicates afforded the 1,2-alkylarylated products. Within the same published work, the Nevado group additionally optimized a carbosulfonylation reaction with similar conditions using conjugated alkene substrates. The proposed mechanism for these reactions is comparable to that proposed by the Chu group.

## Conclusions

In recent years, the surge of developments in nickel-catalyzed intermolecular 1,2-dicarbofunctionalization of alkenes has allowed for the progression of a wide range of elegant strategies toward achieving a general platform for universal alkene difunctionalization. While these notable efforts have laid a strong foundation for the field, several challenges have yet to be overcome. One such challenge is the expansion of the alkene scope. To date, terminal alkene substrates rarely show comparable reactivity in a regio- and stereoselective manner to their more substituted alkene counterparts (*i.e.* 1,1-, 1,2-disubstituted, tetrasubstituted). While strong directing groups enable this type of reactivity, we anticipate that more synthetically relevant functional groups in combination with novel ligand scaffolds will bridge the gap in this chemical space. A second unmet challenge is achieving asymmetric 1,2-dicarbofunctionalization in an intermolecular fashion. In combination with a broader alkene scope, this will undoubtedly serve as a powerful strategy for building complex molecular scaffolds. We anticipate that the combined progress on these and other fronts will ultimately result in complete regio- and stereocontrol in all different types of alkene dicarbofunctionalization.

## Conflicts of interest

The authors declare no conflict of interest.

## Acknowledgements

This work was financially supported by the National Science Foundation (CHE-1800280), the Alfred P. Sloan Fellowship Program, and the Camille Dreyfus Teacher-Scholar Program. We further acknowledge the NSF for Graduate Research Fellowships (DGE-1346837, J. D. and DGE-1842471, O. A.) and the Kwanjeong Educational Foundation for a Graduate Fellowship (T. K.). We thank Raul Martin-Montero for carefully proofreading this manuscript.

## Notes and references

- 1 N. Miyaura and A. Suzuki, *Chem. Rev.*, 1995, **95**, 2457–2483.
- 2 C. C. C. Johansson Seechurn, M. O. Kitching, T. J. Colacot and V. Snieckus, *Angew. Chem., Int. Ed.*, 2012, **51**, 5062–5085.
- 3 For reviews on C(sp<sup>3</sup>)-C(sp<sup>3</sup>) cross-coupling, see: (a) M. R. Netherton and G. C. Fu, *Adv. Synth. Catal.*, 2004, **346**, 1525–1532; (b) A. C. Frisch and M. Beller, *Angew. Chem., Int. Ed.*, 2005, **44**, 674–688; (c) A. Rudolph and M. Lautens, *Angew. Chem., Int. Ed.*, 2009, **48**, 2656–2670; (d) R. Jana, T. P. Pathak and M. S. Sigman, *Chem. Rev.*, 2011, **111**, 1417–1492; (e) X. Hu, *Chem. Sci.*, 2011, **2**, 1867–1886.
- 4 S. Z. Tasker, E. A. Standley and T. F. Jamison, *Nature*, 2014, **509**, 299–309.
- 5 (a) J. B. Diccianni and T. Diao, *Trends Chem.*, 2019, **1**, 830–844; (b) B.-L. Lin, L. Liu, Y. Fu, S.-W. Luo, Q. Chen and Q.-X. Guo, *Organometallics*, 2004, **23**, 2114–2123; (c) V. P. Ananikov, *ACS Catal.*, 2015, **5**, 1964–1971.
- 6 (a) J. Derosa, V. T. Tran, V. A. van der Puyl and K. M. Engle, *Aldrichimica Acta*, 2018, **51**, 21–32; (b) R. Giri and S. KC, *J. Org. Chem.*, 2018, **83**, 3013–3022; (c) J.-S. Zhang, L. Liu, T. Chen and L.-B. Han, *Chem.-Asian J.*, 2018, **13**, 2277–2291.
- 7 For representative examples of 1,2-dicarbofunctionalization with other metals, see: (a) T.-H. Huang, H.-M. Chang, M.-Y. Wu and C.-H. Cheng, *J. Org. Chem.*, 2002, **67**, 99–105; (b) L. Liao, R. Jana, K. B. Urkalan and M. S. Sigman, *J. Am. Chem. Soc.*, 2011, **133**, 5784–5787; (c) K. M. Logan, K. B. Smith and M. K. Brown, *Angew. Chem., Int. Ed.*, 2015, **54**, 5228–5231; (d) J. Terao, Y. Kato and N. Kambe, *Chem.-Asian J.*, 2008, **3**, 1472–1478.
- 8 For representative examples of nickel-catalyzed intramolecular 1,2-dicarbofunctionalization, see: (a) V. B. Phapale, E. Buñuel, M. García-Iglesias and D. J. Cárdenas, *Angew. Chem., Int. Ed.*, 2007, **46**, 8790–8795; (b) S. KC, P. Basnet, S. Thapa, B. Shrestha and R. Giri, *J. Org. Chem.*, 2018, **83**, 2920–2936; (c) K. Wang, Z. Ding, Z. Zhou and W. Kong, *J. Am. Chem. Soc.*, 2018, **140**, 12364–12668; (d) Y.-L. Zheng and S. G. Newman, *Angew. Chem., Int. Ed.*, 2019, **58**, 18159–18164; (e) D. Huang, D. Olivieri, Y. Sun, P. Zhang and T. R. Newhouse, *J. Am. Chem. Soc.*, 2019, **141**, 16249–16254.
- 9 T. Qin, J. Cornella, C. Li, L. R. Malins, J. T. Edwards, S. Kawamura, B. D. Maxwell, M. D. Eastgate and P. S. Baran, *Science*, 2016, **352**, 801–805.
- 10 A. García-Domínguez, Z. Li and C. Nevado, *J. Am. Chem. Soc.*, 2017, **139**, 6835–6838.



- 11 W. Shu, A. García-Domínguez, M. T. Quiróz, R. Mondal, D. J. Cárdenas and C. Nevado, *J. Am. Chem. Soc.*, 2019, **141**, 13812–13821.
- 12 J.-W. Gu, Q.-Q. Min, L.-C. Yu and X. Zhang, *Angew. Chem., Int. Ed.*, 2016, **55**, 12270–12274.
- 13 Z.-F. Yang, C. Xu, X. Zheng and X. Zhang, *Chem. Commun.*, 2020, **56**, 2642–2645.
- 14 C. Xu, Z. F. Yang, L. An and X. Zhang, *ACS Catal.*, 2019, **9**, 8224–8229.
- 15 M. Chierchia, P. Xu, G. J. Lovinger and J. P. Morken, *Angew. Chem., Int. Ed.*, 2019, **58**, 14245–14249.
- 16 G. J. Lovinger and J. P. Morken, *Eur. J. Org. Chem.*, 2019, DOI: 10.1002/ejoc.201901600.
- 17 (a) M. W. Campbell, J. S. Compton, C. B. Kelly and G. A. Molander, *J. Am. Chem. Soc.*, 2019, **141**, 20069–20078; (b) S.-Z. Sun, Y. Duan, R. S. Mega, R. J. Somerville and R. Martin, *Angew. Chem., Int. Ed.*, 2020, **59**, 4370–4374; (c) R. S. Mega, V. K. Duong, A. Noble and V. K. Aggarwal, *Angew. Chem., Int. Ed.*, 2020, **59**, 4375–4379.
- 18 (a) G. J. Lovinger and J. P. Morken, *J. Am. Chem. Soc.*, 2017, **139**, 17293–17296; (b) S. M. Koo, A. J. Vendola, S. N. Momm and J. P. Morken, *Org. Lett.*, 2020, **22**, 666–669.
- 19 B. Shrestha, P. Basnet, R. K. Dhungana, S. KC, S. Thapa, J. M. Sears and R. Giri, *J. Am. Chem. Soc.*, 2017, **139**, 10653–10656.
- 20 S. Thapa, R. K. Dhungana, R. T. Magar, B. Shrestha, S. KC and R. Giri, *Chem. Sci.*, 2018, **9**, 904–909.
- 21 S. KC, R. K. Dhungana, B. Shrestha, S. Thapa, N. Khanal, P. Basnet, R. W. Lebrun and R. Giri, *J. Am. Chem. Soc.*, 2018, **140**, 9801–9805.
- 22 S. KC, R. K. Dhungana, V. Aryal and R. Giri, *Org. Process Res. Dev.*, 2019, **23**, 1686–1694.
- 23 P. Gao, L.-A. Chen and M. K. Brown, *J. Am. Chem. Soc.*, 2018, **140**, 10653–10657.
- 24 D. Anthony, Q. Lin, J. Baudet and T. Diao, *Angew. Chem., Int. Ed.*, 2019, **58**, 3198–3202.
- 25 A. A. Kadam, T. L. Metz, Y. Qian and L. M. Stanley, *ACS Catal.*, 2019, **9**, 5651–5656.
- 26 J. Derosa, V. T. Tran, M. N. Boulous, J. S. Chen and K. M. Engle, *J. Am. Chem. Soc.*, 2017, **139**, 10657–10660.
- 27 J. Derosa, V. A. van der Puyl, V. T. Tran, M. Liu and K. M. Engle, *Chem. Sci.*, 2018, **9**, 5278–5283.
- 28 V. A. van der Puyl, J. Derosa and K. M. Engle, *ACS Catal.*, 2019, **9**, 224–229.
- 29 R. Pan, C. Shi, D. Zhang, Y. Tian, S. Guo, H. Yao and A. Lin, *Org. Lett.*, 2019, **21**, 8915–8920.
- 30 W. Li, J. K. Boon and Y. Zhao, *Chem. Sci.*, 2018, **9**, 600–607.
- 31 P. Basnet, R. K. Dhungana, S. Thapa, B. Shrestha, S. KC, J. M. Sears and R. Giri, *J. Am. Chem. Soc.*, 2018, **140**, 7782–7786.
- 32 P. Basnet, S. KC, R. K. Dhungana, B. Shrestha, T. J. Boyle and R. Giri, *J. Am. Chem. Soc.*, 2018, **140**, 15586–15590.
- 33 R. K. Dhungana, S. KC, P. Basnet, V. Aryal, L. J. Chesley and R. Giri, *ACS Catal.*, 2019, **9**, 10887–10893.
- 34 X. Zhao, H.-Y. Tu, L. Guo, S. Zhu, F.-L. Qing and L. Chu, *Nat. Commun.*, 2018, **9**, 3488.
- 35 J. Derosa, R. Kleinmans, V. T. Tran, M. K. Karunananda, S. R. Wisniewski, M. D. Eastgate and K. M. Engle, *J. Am. Chem. Soc.*, 2018, **140**, 17878–17883.
- 36 V. T. Tran, Z. Li, T. J. Gallagher, J. Derosa, P. Liu and K. M. Engle, *Angew. Chem., Int. Ed.*, 2020, DOI: 10.1002/anie.201915454.
- 37 J. Derosa, T. Kang, V. T. Tran, S. R. Wisniewski, M. K. Karunananda, T. C. Jenkins, K. L. Xu and K. M. Engle, *Angew. Chem., Int. Ed.*, 2020, **58**, 1202–1205.
- 38 L. Guo, H.-Y. Tu, S. Zhu and L. Chu, *Org. Lett.*, 2019, **21**, 4771–4776.
- 39 A. García-Domínguez, R. Mondal and C. Nevado, *Angew. Chem., Int. Ed.*, 2019, **58**, 12286–12290.

